No, Not That Way, the Other Way: Creating Active Sites in Self-Assembled Host Molecules

Richard J. Hooley*[a]

[a] Department of Chemistry and the UCR Center for Catalysis, University of California-Riverside, 501 Big Springs Road, Riverside, CA 92521, U.S.A.

richard.hooley@ucr.edu

Dedicated to Prof. Julius Rebek, Jr., on the occasion of his 75th birthday.

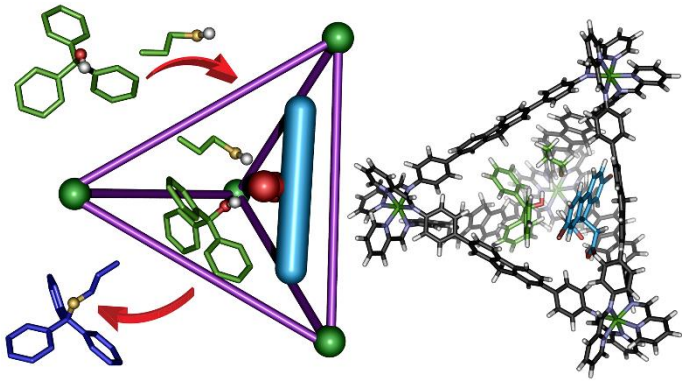

Received:
Accepted:
Published online:
DOI:

Abstract This Account describes our efforts over the last decade to synthesize self-assembled metal-ligand cage complexes that display reactive functional groups on their interiors. This journey has taken us down a variety of research avenues, including studying the mechanism of reversible self-assembly, analyzing ligand self-sorting properties, post-assembly reactivity, molecular recognition and binding studies, and finally reactivity and catalysis. Each of these individual topics are discussed here, as are the lessons learned along the way and the future research outlook. These self-assembled hosts are the closest mimics of enzymes to date, as they are capable of size- and shape-selective molecular recognition, substrate activation and turnover, as well as showing less common "biomimetic" properties such as the ability to employ cofactors in reactivity, and alter the prevailing mechanism of the catalyzed reactions.

Key words Molecular Recognition • Enzyme Mimicry • Self-Assembly • Catalysis • Coordination Complexes • Host:Guest Chemistry

I. Introduction

Whenever I first meet a student interested in our research on "enzyme-mimicking catalysis" for the first time, I ask one question: what is the difference between a small molecule catalyst and an enzyme? Most of the answers end up with some variation on "enzymes are more efficient catalysts". This is mostly true, but misses the point. What is the point of attempting to create large, complex, unwieldy macromolecules if the goal is to do what simple catalysts can do, just a little bit better? My answer is twofold: discovery of unknown behavior is always interesting, but also, let's attempt to find reactivity that *cannot* be achieved by small molecule catalysts. The key to that lies in molecular recognition.

Our work over the last decade has focused, in quite a broad way, on solving this problem, and attempting to create "host" molecules that can display functional groups to their substrates, controlling their recognition and reactivity. This simple concept belies a complex series of requirements. The host must be a "host", which means that a defined, spacious cavity is required that provides some favorable interactions to the guest to entice it inside. The functional groups must be oriented internally, not externally, and must not occupy the space inside the host, which would prevent guest binding. The host must be soluble, stable, and tolerant to reaction conditions. It would also be helpful if it were relatively symmetrical, to ease analysis by NMR spectroscopy and allow single crystal growth, to please reviewers. Finally, it must be functional and allow turnover: plenty of hosts are known that simply bind guests,[1] but enzymes bind substrates, convert them into products, and then release those products. All of these requirements must be satisfied, and some are not trivial.

This, then, leads to the question of how to go about this: what kind of strategy is appropriate? There are a wide range of host macrocycles in the literature,[2] including simple bowl-like or toroidal hosts, and all the principles of "artificial enzyme" catalysis were illustrated with these systems many years ago.[3] They rely on pre-organization of the reactive groups, though, and do not have defined 3D cavity architectures.[4] Fully enclosed capsules have been known for almost as long: Cram created some spectacular covalent spheroids over 30 years ago,[5] but the synthetic challenge in making derivatized carcerands and hemicarcerands is high. Rebek used weak forces such as hydrogen bonds to form reversible capsules,[6] and Gibb has used the hydrophobic effect to make capsules in aqueous solution,[7] but none of these hosts are easily tunable to allow internal functions into the active site. Rebek's deep cavitands[8] do allow reactive functions to be presented to bound guests, and a variety of interesting behavior was seen with internal acid and aldehyde groups, such as increased reactivity,[9] size-selectivity[10] and the stabilization of reactive intermediates.[11] These hosts provided the inspiration for my independent career, and a target to aim for. However, having worked with the internalized aldehyde cavitand as a postdoc, it was clear that trying to create derivatized

cavitands was not a suitable path for an Assistant Professor who wanted to publish anything anytime soon. Metal-ligand self-assembly seemed like an easy way to some quick results. Raymond[12] and Fujita[13] were publishing scores of papers on the reactions and properties of self-assembled metal-ligand cage complexes. In the words of a certain well-known UK tv host, "How hard could it be"?

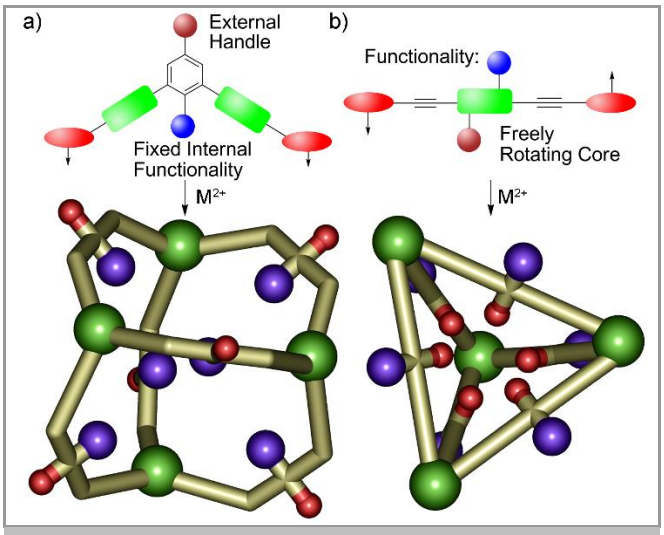

Figure 1. Strategies to allow construction of self-assembled cage complexes with internalized functional groups.

The first task was to make a self-assembled cage complex with internalized groups, and determine whether it would be a good scaffold for further experimentation. The synthetic strategy required three components: a central core containing functional groups for internalization, rigid spacers to lengthen the ligand and allow a sufficiently sizable cavity, and metal-coordinating groups at the ligand termini to allow reversible self-assembly. We originally had two general ideas of how to do this (Figure 1), either use V-shaped ligands that force a reactive group to the cavity interior (as opposed to the outside), or use a linear ligand with functional groups that can freely rotate, which removes the problem of internal vs external orientation. Other groups have exploited each of these concepts while we have been pursuing this project: Fujita has created some beautiful nanostructures with variably decorated internal spaces (Figure 2a-b).[14] These cages differ from our targets in that they have very large cavity volumes, so selective molecular recognition of single small molecules is a challenge. These systems are better described as different "phases" in a reaction flask,[15] rather than active site mimics, but they have recently proven very successful as biomimetic catalysts, as shown by both Fujita[16] and Reek (Figure 2d).[17] Nitschke has created a large number of polyhedral assemblies, and one notable cage (Figure 2c) is a good example of the rotor concept, showing accelerated phosphonate solvolysis abilities.[18]

These strategies are quite general, though, and there are numerous challenges that need to be considered. Reactive functional groups are, by definition, not inert, and can interfere with the self-assembly process, either due to steric effects (filling the internal cavity, preventing guest binding) or because of incompatibility with the M-L contacts. The type of M-L contact is important - it needs to be robust enough to survive the desired reaction, but flexible enough to allow reversible self-assembly. In addition, stereochemistry is a serious issue: does adding the reactive groups to the ligand introduce stereocenters? Does the assembly create metal-centered stereoisomers? And can multiple different ligands be incorporated in the assembly, to allow different reactive functions to be incorporated? All of these concepts must be considered when planning a target, not to mention "obvious" problems such as synthetic accessibility, solubility and substrate binding affinity and turnover. Each of these challenges arose at certain times during the initial stages of this project, which explains why it is still ongoing…

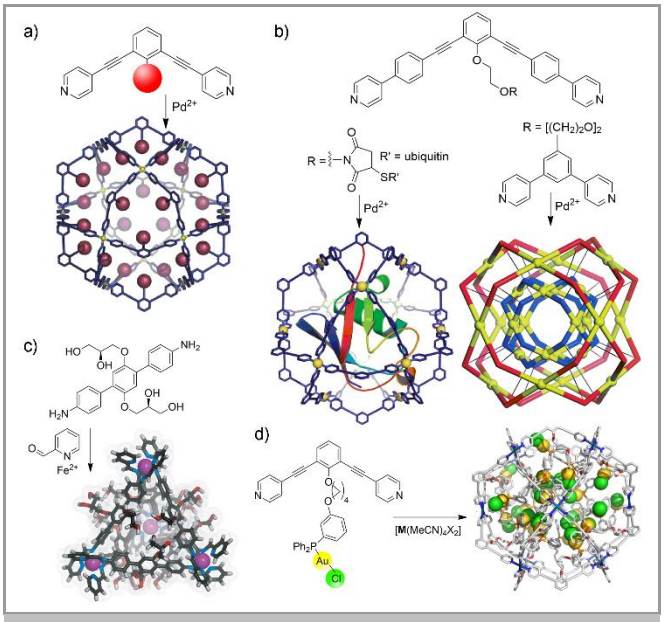

Figure 2. Literature examples of internally functionalized self-assembled cages. a) Pd-mediated $M_{12}L_{24}$ nanospheres;[15] b) application of the $M_{12}L_{24}$ cages to internalize proteins or other cages;[14c,14d] c) Fe-iminopyridine cages with rotor ligands;[16] d) catalytic $Pd_{12}L_{24}$ cages.[17]

II. Paddlewheels and Self-sorting Behavior

Our initial attempts relied on precedented methods of internalizing functional groups, mainly to provide a quick result. Using an aromatic ring with a functional group directly between two alkynylpyridine units (Figure 2a) forces the functionality to the cavity interior when combined with Pd-pyridyl coordination to form large assemblies.[14] However, we required a smaller cage assembly than Fujita's $M_{12}L_{24}$ nanospheres, so we simply varied the coordination angle of the pyridyl units from para to meta (Figure 3). With acetylene units as spacers, the free rotation of the pyridyl unit could allow formation of coordination polymers or discrete M_2L_4 paddlewheel assemblies, as had been shown by Puddephatt[19] (and later exploited by Crowley[20] and Clever,[21] among others, to make some beautiful interpenetrated assemblies). Our questions were simple: can the assembly process tolerate reactive functional groups on the interior, and how are the assemblies affected by the presence of internal groups in a tightly packed interior?

The simple paddlewheel **1a** (i.e. Pd_2**L1a**$_4$) is easily made by mixing ligand **L1a** and $Pd(NO_3)_2$ in DMSO. Formation is rapid, and the assembly is stable in air and at room temperature. Crystallographic analysis of the triflate salt shows that one triflate anion was bound in the cavity interior, and that there was

sufficient space available to bind guests such as terphthalonitrile.[22] The nitrate and triflate salts are only soluble in DMSO, which is a competitive guest and limits its applications. By changing counterions, the cage can be solubilized in more desirable solvents, and Lusby has shown some beautiful examples of supramolecular Diels-Alder catalysis with this cage system.[23]

The cavity size is such that other groups can be positioned on the interior of the paddlewheel structure, including amino groups. Interestingly, the self-assembly of amino ligand **L1b** is successful, and the internal $-NH_2$ groups are completely ignored by the Pd centers, which coordinate only to the terminal pyridines. The crystal structure of **1b** is notably different to the unfunctionalized **1a** equivalent, however. The triflate anion on the interior of the paddlewheel repels the amino groups, causing a twisting of the M_2L_4 structure: the individual cage structures are quite similar, merely having different coordination angles, but this twist causes the unit cell packing to be quite different (Figure 3b).[24]

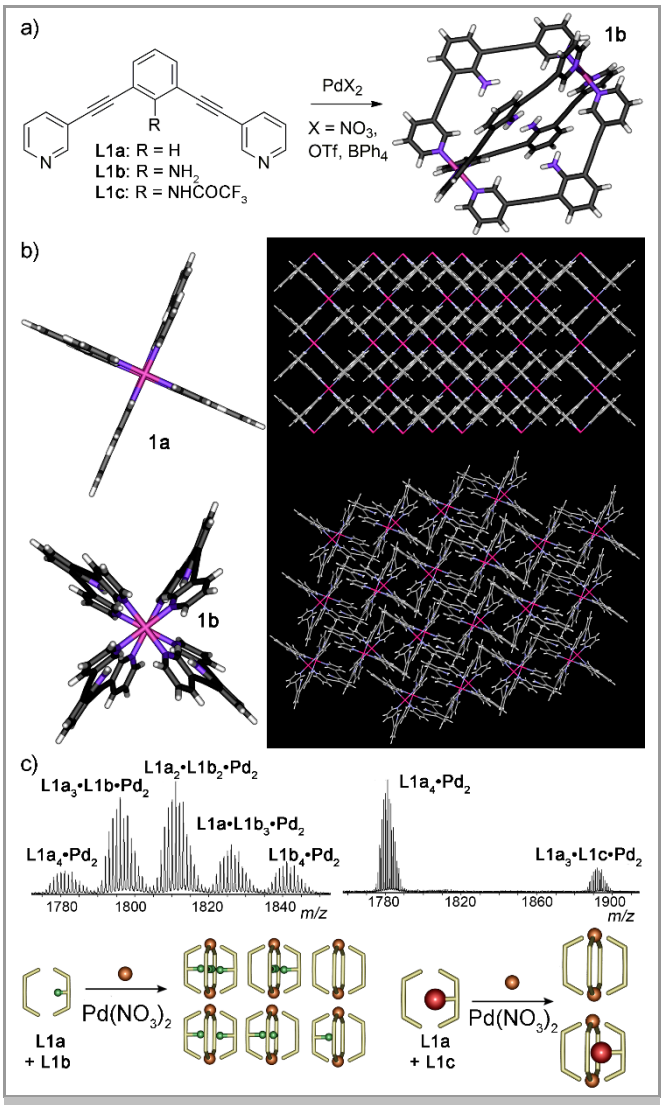

Figure 3. a) Self-assembly of internally functionalized Pd_2L_4 paddlewheel complexes; b) crystal structures of cages **1a** and **1b**;[22,24] c) self-sorting in Pd_2L_4 paddlewheel complexes.[25]

Increasing the size of the internal group provides some interesting possibilities in self-sorting. Ligand **L1c** has an internal trifluoroacetamide group: when that ligand is combined with $Pd(NO_3)_2$, an undefined aggregate is formed, as the interior cavity space in the paddlewheel is too small to fit four trifluoroacetamide groups. It is large enough, however, to fit one: when ligands **L1a** and **L1c** are added at the same time to a solution of $Pd(NO_3)_2$, a single heterocomplex **L1a$_3$•L1c•Pd$_2$** is formed (along with Pd_2**L1a$_4$**). This selectivity is based on sterics: only one $NHCOCF_3$ group can be internalized. When the smaller amino-functionalized ligand **L1b** is used in concert with **L1a**, no selectivity is observed, and a statistical mixture of all isomer possibilities is formed.[25] If an even larger group is used (N-phenylurea), then no assembly is possible even in the presence of **L1a**.

While the self-sorting behavior was interesting, our goal with the M_2L_4 assemblies was to see whether the Pd-pyridyl coordination could outcompete non-specific binding to an amine group, and technically speaking, this was successful. However, the NH_2 in ligand **L1b** is so electron poor, it is essentially unreactive (trifluoroacetylation is about its limit), so this system was not going to satisfy our central goal. In addition, the limited solubility, and sensitivity to external ions such as chloride were also problematic factors, so we decided to focus on different modes of assembly. It is worth noting that a number of other groups have gone on to use the Pd_2L_4 motif for biomimetic catalysis,[26] molecular recognition,[27] and many other applications that are far more impressive,[28] so this was a case of leaving an area too soon.

III. Octahedral Transition Metal-mediated Assembly: Sorting and Stereochemical Control

As the Pd-pyridyl coordination motif didn't appear promising (to us), we shifted focus and attempted to synthesize different, novel coordinating motifs that would both move towards the main goal and provide some interesting new types of assembly. Greater robustness in the metal-ligand coordination was needed. There are several different metal-ligand coordination strategies in the literature, and we investigated a large number of them, and made a lot of insoluble products. Some strategies were more successful, though, notably self-assemblies formed from salicylhydrazide ligands and lanthanide ions.[29,30] Lanthanide-mediated assembly has many advantages, including the formation of chiral,[31] luminescent,[32] and photoreactive cages.[33] Our particular coordination motif is excellent at conferring selectivity on small assemblies,[29] but the highly anionic nature of the salicylhydrazide group proved challenging to extend to larger assemblies. We did make some M_4L_6 assemblies with linear bis-salicylhydrazide ligands,[30] but their lack of solubility rendered them impractical for host:guest studies.

Of course, the obvious solution is to use octahedral transition metals for assembly. The reason we were a little reticent to do this is simply a fear of being "scooped". The scope and function of cage complexes that use octahedral transition metal ions has been quite effectively strip-mined, originally by the Raymond/Bergman groups with catecholate ligands,[34] and subsequently by the Nitschke group with metal-iminopyridine assemblies.[35] But, spectacular as their work has been, we felt that the application of internal functionality was still an underexplored area, and we were quite excited to use a metal-ligand coordination system that provided cages that were well-behaved and soluble.

Combining amines, formylpyridines and metal salts to reversibly form cage complexes was originally pioneered by Hannon,[36] and has been popularized to an impressive extent by Nitschke.[37] The multicomponent assembly process is quite simple (Figure 4). Mixing the various components in a solvent, usually CH_3CN, followed by heating (in most cases), yields the thermodynamically most stable product, the structure of which is dependent on the ligand coordination angle (among other things). A wide range of polyhedral shapes are possible, but for our purposes, we focused on linear diamines, which tend to form M_4L_6 tetrahedra,[38] or bent, V-shaped diamines, which favor the smaller M_2L_3 helicate structures.[39] The metal ions smooth the imine formation process, the resulting cages are nicely soluble in organic solvents, and even can be dissolved in water with some modifications to the ligand or metal counterion used.[40]

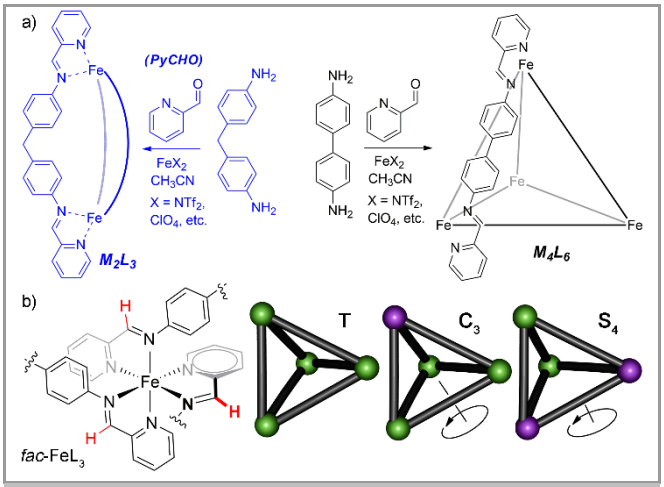

Figure 4. Fe-iminopyridine complexes. a) Simple stoichiometries of assembly; b) stereochemical outcomes in M_4L_6 assembly.[42]

Using octahedral transition metals introduces a new challenge to the assembly process: metal-centered stereoisomers.[41] This was not a concern when using square-planar Pd^{2+} or with Ln^{3+} ions, which maintained some solvent-coordinated sites after assembly.[29] However, using multiple octahedral metals in an assembly introduces the possibility of stereoisomeric cages. This area has been deeply investigated for Ga-catecholate ligands[12a] and Fe-iminopyridine systems.[42] Octahedral metal centers with dissymmetric ligands can adopt three stereoisomers, either facial (*fac*), which can form two enantiomeric isomers Λ, Δ, or meridional (*mer*).[43] The vast majority of M-L complexes have *fac* metal centers, but controlling the Λ/Δ isomerism can be more challenging. The short takeaway from Raymond and Nitschke's extensive studies is that highly rigid ligands are able to control the relative stereochemistry at the metal centers, whereas more flexible ones form a mixture of isomers.

Our first attempt to create internally functionalized complexes exploited variants of ligands used for the Pd-pyridyl assembly process (Figure 5a).[44] Combination of the diamines **L2a** or **L2b** with 2-formylpyridine (PyCHO) and $Fe(ClO_4)_2$ in CD_3CN formed M_2L_3 helicate structures with internalized groups. These complexes were not particularly stable, but did provide an interesting effect on stereochemistry. The ligand **L2a** is quite flexible, and forms a 50:50 mixture of ΛΛ/ΔΔ and ΔΛ diastereoisomers upon assembly. If ligand **L2b** is used, the large benzyloxy groups completely pack the interior of the helicate, introducing additional strain on the assembly. This affects the stereoselectivity at the metals, yielding only the matched ΛΛ/ΔΔ diastereoisomer.

Of course, our goal was to introduce *functional* groups to these systems (as opposed to simple space-filling groups), and the ligand **L2** scaffold was not simple to derivatize. We investigated other methods of internalizing functionality, and came across another issue: how would *ligand-based* stereocenters affect the self-assembly process, and could any selectivity be conferred on the assembly? To test this, a series of diaminodibenzosuberyl ligands **L3-L5** were synthesized with varying internal groups, and subjected to multicomponent self-assembly with PyCHO and Fe^{II} salts.[45] The slightly bent ligands form M_2L_3 *meso*-helicates, with each metal center displaying *fac* orientation.

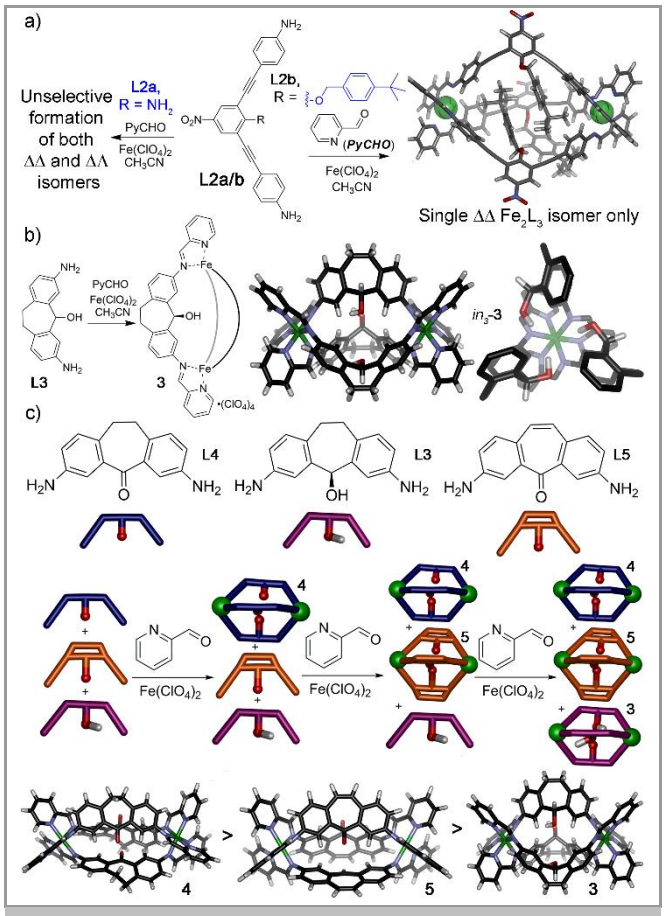

Figure 5. a) Control of metal-based stereochemistry *via* internal packing;[44] b) internal H-bonds control ligand stereochemistry in M_2L_3 *meso*-helicates;[45] c) narcissistic self-sorting of highly similar ligands in helicate assembly.[46]

The most interesting example is the suberol-based complex **3** (Figure 5b), which has the potential to form four different ligand-centered diastereomers, irrespective of any metal-centered isomerism. As the Fe centers are chiral, the prochiral –CHOH group on the ligand can adopt two configurations upon assembly, either "in", towards the center of the helicate, or "out". As there are three ligands in the assembly, four isomers are possible, in_3, in_2out, out_2in and out_3. Interestingly, complex **3** shows only a single isomer in solution, with the in_3 orientation. There are minimal steric differences between the three isomers, but the all-in isomer can take advantage of interligand H-bonding (Figure 5b), which the other conformations cannot. Reversible self-

assembled systems exploit multiple weak forces between metals and coordinating ligands upon formation, which is why entropically disfavored multicomponent assemblies can be accessed under mild conditions. Those forces favor the formation of the assemblies as a whole: 11 components (three diamines, six aldehydes and two metal ions) combine to form M_2L_3 helicates for all suberyl ligands tested. The hydrogen bonding adds a second layer of selectivity that allows discrimination between different isomers of the assemblies. This is reminiscent of protein folding, where favorable structural factors combine with multiple H-bonds to select between a variety of local minima. In the case of complexes **3-5**, only the alcohol ligands show diastereoselectivity via favorable H-bonding: if the –OH groups are replaced with ethers, then a statistical mixture of all 4 isomers is seen. If the H-bond donor atoms are further away from each other in the assembly (R = OCONHBu), then favorable interligand H-bonding cannot occur, and all four isomers are seen.[44] Only when the H-bonds are perfectly positioned can diastereoselectivity occur.

The selectivity in helicate formation is dependent on a number of factors, including H-bonding, and these Fe-iminopyridine complexes show much greater self-sorting abilities between ligands than the Pd_2L_4 paddlewheels shown earlier. Three ligands were tested that, at first glance, are extremely similar in structure: diamino-suberone **L4**, -suberenone **L5**, and -suberol **L3**. When combined with PyCHO, each of the ligands forms the expected M_2L_3 *meso*-helicate structures (Figure 5c). When mixed together in the same reaction vessel, though, high degrees of narcissistic self-sorting were observed.[46] When combining different ligands in self-assembly processes, two types of self-sorting are possible: social, whereby different ligands are embedded in the same assembly to form heterocomplexes,[47] or narcissistic, where only homocomplexes are formed.[48] When the coordinating groups are different, self-sorting is simple to control, and only the correct "matched" coordinators can pair up. This is well-known for H-bonding systems[49] and metal-ligand assemblies,[50] and both types of sorting are possible. In our case, however, the coordinating groups are identical iminopyridine units, and there is essentially no electronic/donor difference between the ligands. As such, any ligand self-sorting relies on other factors. The pyridyl ligands **L1a-L1b** showed the "expected" outcomes, whereby ligands with identical coordinating groups form statistical mixtures of heterocomplexes (Figure 3c), with no selectivity seen, and only when the interior cavity was packed did any discrimination occur. Even then, complete selectivity was not possible.

The reasons for the high fidelity narcissistic self-sorting of **3-5** are still not completely clear, but DFT minimization of the complexes sheds some light on the selectivity. When forming the helicates, the diaminosuberyl ligands must be bent out of plane to form the assembly. There is an entropic penalty to this process too, due to additional rigidification of the ligand upon formation of the helicate. Suberone ligand **L4** incurs the lowest penalty to deformation, followed by the more rigid suberenone **L5**, and finally the suberol **L3**. This was surprising, as the suberol ligand had shown diastereoselectivity upon assembly due to favorable internal H-bonding. This beneficial H-bonding was not enough to outweigh the penalty for backbone deformation, however, and the suberol ligand proved the least stable of the three complexes.[46]

This self-sorting order was further illustrated by *subcomponent exchange*, whereby some of the ligand components in an intact cage can be replaced by components of different structure.[51] Post-assembly exchange was possible by adding diamine to a preformed cage complex. In each case, the most favored prevailed, so addition of diaminosuberol **L3** to suberone cage **4** gave no reaction, but diaminosuberone **L4** could displace the ligand from suberol cage **3** in <1 h at 50 °C. Interestingly, the *aldehyde* component can also be exchanged.[52] This was unexpected: the mechanism of diamine exchange with a metal-coordinated imine is very simple, as the nucleophile adds into the electron withdrawn C=N bond. If an aldehyde is added to a preformed cage, no reaction should occur, as there is no nucleophile in the system: all the $-NH_2$ groups are occupied as imines. However, if a small amount of water is added to "grease the wheels", aldehyde subcomponent exchange is possible, presumably via a transient solvolysis of the iminopyridine, which allows equilibration to the most favored species. More strongly donating aldehydes are more favored, so 2-formylpyridine can displace 5-bromo-2-formylpyridine, but not the other way around. Again, it should be noted here that the Nitschke lab has performed an extensive series of studies on these processes in larger, more complex systems as well.[53]

2-Formylpyridines with groups at the 5-position have no steric clash with the metal centers, and any differences in assembly are merely based on donor ability. If species such as 6-methyl formylpyridine (MePyCHO) are used (or 2-formylquinoline), the assembly behavior is quite different.[52,54] The packing around the Fe centers is much more challenging, and any complexes formed are not diamagnetic, but are *paramagnetic*, with high spin Fe centers (Figure 6).[55] The increased bulk around the pyridyl centers forces two changes to the coordination environment, allowing the assembly of three methylpyridines around each Fe center. The Fe-N bond lengths are increased by ~0.2 Å, and significant twisting of the ligands occurs, so the N-Fe-N bond angles are deviated from the standard octahedral arrangement to angles of ~75° and ~108°, depending on the specific helicate formed. These twisted ligand angles and longer bond distances favor high spin Fe^{II}, and the resulting complexes show ^{1}H NMR signals ranging from δ -100 ppm to +190 ppm. The relative favorability of the assemblies is altered as well. As there is a need to adopt far more twisted bond angles in the helicate assembly, more flexible diamine ligands are more favored, so diaminosuberol **L3** is capable of forming paramagnetic helicates with both MePyCHO and 2-formylquinoline. However, diaminosuberone **L4**, which was by far the most successful diamine core for helicate formation with PyCHO, is too rigid, and is incapable of forming helicates with MePyCHO at all (Figure 6a).

The paramagnetic helicates are, in general, less stable than the diamagnetic versions, which allows the magnetism to be "switched off" by subcomponent exchange. Aldehyde subcomponent exchange is only successful if the product is more stable than the starting cage, so if PyCHO is added to a solution of paramagnetic cage **3•Me** with a small amount of water, then the more favorable cage **3•H** can be formed after heating. The intermediates of the reaction can be observed in the ^{1}H NMR as individual PyCHO groups replace their MePyCHO counterparts

(Figure 6c). Interestingly, the presence of only three MePy groups in the assembly (out of a total of 6) are necessary to confer paramagnetism on the helicate. Once three aldehydes switch out (on average), the overall high spin nature of the Fe centers is lost and the magnet is "turned off". Unfortunately, the process is only unidirectional: as the paramagnetic helicates are less stable than their diamagnetic equivalents, we haven't yet found a way to go uphill and turn the magnets on. But we are still trying.

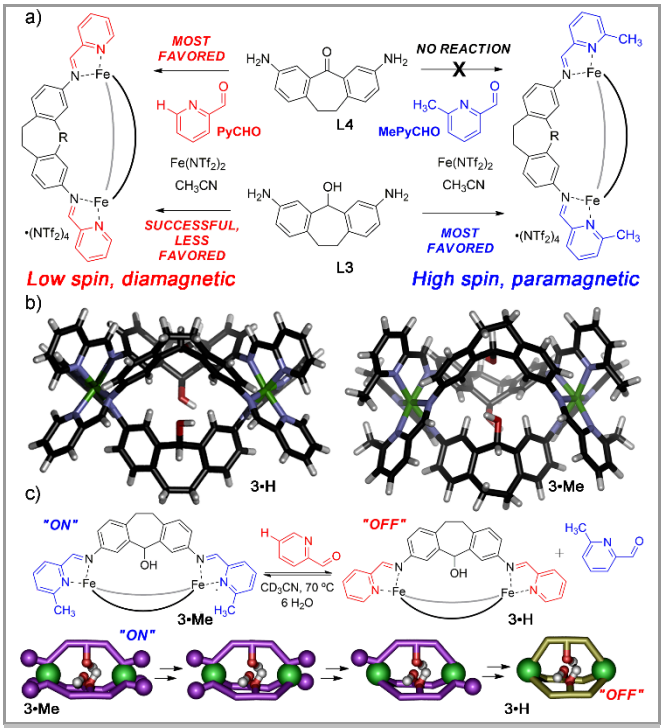

Figure 6. a) Assembly of diamagnetic or paramagnetic helicates upon aldehyde terminus variation; b) structures of diamagnetic helicate **3•H** and paramagnetic helicate **3•Me**; c) "switch-off" paramagnetism *via* subcomponent exchange.[55]

The M_2L_3 *meso*-helicate complexes are easy to analyze, and provide a wealth of interesting studies in selectivity, sorting and reactivity. But they are small, have no cavity, and can never be enzyme-mimicking catalysts. Somehow, we need to create larger, M_4L_6 systems with an internal cavity. While the 7-membered central ring in **3-5** creates a "V-shaped" diamine ligand, 2,7-diaminofluorenol **L6** is far more linear, and is unlikely to be able to form an M_2L_3 complex upon assembly. Linear diamine ligands are well-known to favor M_4L_6 assemblies upon reaction with Fe^{II} and PyCHO,[42a] and there are (generally) two common stereochemical outcomes of those reactions. The metal centers almost always favor the all-*fac* orientation, leading to two types of stereoisomerism. Short, rigid diamines such as benzidine form single *T*-symmetric diastereomers with ΛΛΛΛ/ΔΔΔΔ configurations at the metal centers.[42] If the ligand is lengthened (e.g. *para*-diaminoterphenyl), stereochemical communication between metal centers is reduced, and a mixture of *T*, S_4 and C_3 isomers is formed, with the proportions depending on the nature of the ligand (Figure 4).[42] Notably, these ligands do not contain ligand-based stereocenters as well, because that exponentially increases the number of possible isomers in the cage. The assembly of diaminofluorenol **L6** could conceivably have Λ-*fac*, Δ-*fac*, or *mer* configurations at each of the four metal centers, as well as two orientations of the OH group at each of the six prochiral ligands. Suffice it to say, that's a lot of isomeric possibilities, and this was one of those times as a PI where you tell your student not to even bother with the experiment. Full credit to Mike Young, though, he tested it anyway, and the resulting cage was extremely unusual. The assembly is highly diastereoselective, and >95% of one single diastereomer is formed,[56] (Figure 7a). The metal centers adopt an unusual *mer₃fac* configuration, which allows the –OH groups to participate in two types of favorable H-bonding: both interligand H-bonds between OH groups and OH-anion interactions with an encapsulated ClO_4^- ion. This makes the ^1H NMR quite complex, because the cage is dissymmetric, and many of the protons in the ligand are non-equivalent. Still, the spectrum is sharp and can be assigned (albeit with difficulty). The assembly requires a properly shaped templating anion: BF_4^- is a successful template, but reaction in the presence of larger ions such as triflate, Ph_2SiF_3-, and BPh_4^- gives an undefined aggregate. Interestingly, as the assembly process is reversible, the cage can be reformed from the aggregate by heating in the presence of Bu_4NClO_4, illustrating the favorability of the H-bonding process.

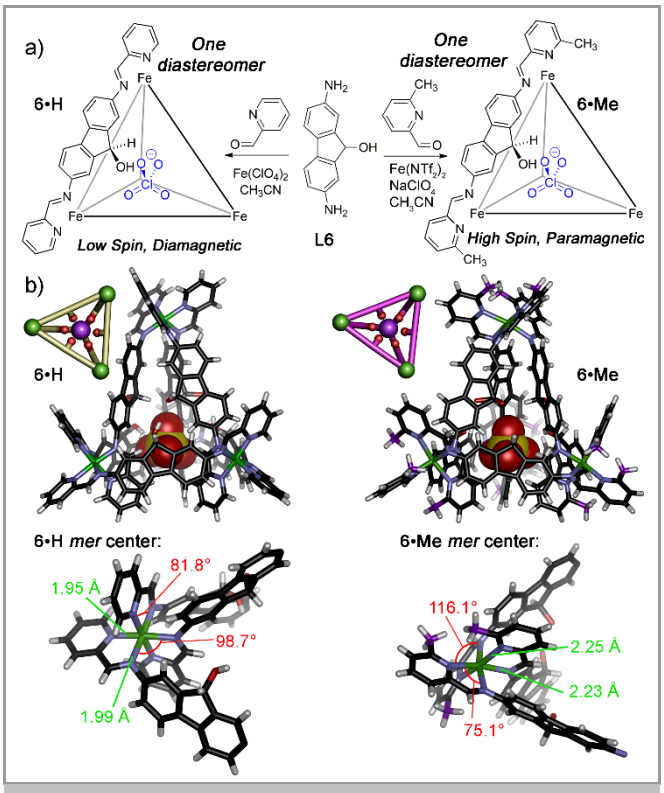

Figure 7. a) H-bonding and anion templation allow diastereoselectivity in M_4L_6 cage assembly;[56,55] b) differences in the coordination environment at the *mer* centers in **6•H** and **6•Me**.[55]

The *mer₃fac* stereochemistry at the metals is also very useful for creating paramagnetic assemblies.[55] Even though the diaminofluorenol ligand is very rigid (and therefore should not be amenable to assembly with MePyCHO), the highly twisted coordination angles at the *mer* centers in **6** are already perfectly positioned to incorporate more steric bulk (Figure 7b). Paramagnetic cage **6•Me** forms very easily when **6•H** is heated with MePyCHO and $Fe(ClO_4)_2$ in CH_3CN, and shows NMR peaks in the characteristic δ -100 ppm to +200 ppm region. The wide spread of the spectral range is actually useful in assigning the spectrum, as more peaks can be distinguished than in the

diamagnetic case. Crystallographic analysis of this complex was far more challenging, however. ClO_4 salts of iminopyridine cages are less soluble than their NTf_2 counterparts, so single crystals are almost always more accessible as triflimide salts. The problem is that ClO_4^- is needed to template the assembly of **6**, so simply using the triflimide was never going to work. After a lot of experimentation, Lauren Holloway managed to grow crystals of a mixed NTf_2/ClO_4 salt, and the structure shown in Figure 7b could be solved (full credit to Dr. Fook Tham for that).

IV. Post-Assembly Reactivity

The next question to be asked, after the cages have been made, is what can you do with them? Can you perform reactions on them? Can you perform reactions *with them*? Reversible self-assembled cages are often compared to solid-state metal organic frameworks, as they have many of the same applications in molecular recognition. When it comes to post-assembly reactivity, however, self-assembled cages behave far differently. Subcomponent exchange was discussed before, and is usually very easy: the reversible nature of the Fe-iminopyridine vertices is perfectly suited to transimination reactions, and this has been used in a variety of applications.

On the other hand, *subcomponent transformation* involves new bond forming reactions on the ligand backbone of an intact cage. This is very simple with MOFs,[57] but far more challenging with reversible cages. Still, there are a number of examples of subcomponent transformation,[58] but many of them involve neutral reactants. Nitschke has shown some beautiful examples of post-assembly reactivity using pericyclic reactions,[59] including some processes that actually switch between cage stoichiometries.[60] These reactions illustrate the point: while spectacular, they only require heat to occur, side-stepping the main issue with adding nucleophilic reactants to Fe-iminopyridine cages. We were interested in polar reactions: can we perform nucleophilic substitutions at the ligand backbone? The first example was with suberol helicate **3**: this cage can be reacted with isocyanates after assembly, converting the alcohols to carbamate groups.[45] The process is accelerated by intra-cage H-bonds (when compared to reaction of suberol ligand surrogates with isocyanates in free solution), and an interesting stereochemical outcome is observed. Whereas suberol cage **3** is a single diastereomer, conversion to the corresponding carbamate changes the nature of the H-bonding groups, removing any intra-cage interactions, and four isomers are seen.

While interesting, that reaction was very easy, with no exogenous nucleophiles. A more stringent test would be a nucleophilic displacement reaction. We synthesized the doubly activated chloro ligand **L7** (Figure 8a), and attempted form a helicate from that, with the intention of performing a nucleophilic substitution at the CHCl center.[61] Interestingly, diaminosuberyl chloride **L7** did not form a helicate complex when reacted with PyCHO and $Fe(ClO_4)_2$. The reactive alkyl chloride group is intact and does not react under the assembly conditions, but the product is a disordered aggregate, rather than a defined helicate. The exact structure of the aggregate **7** is unclear, but it displays all the characteristics of a diamagnetic Fe-iminopyridine assembly, and is most likely a coordination polymer. It is not obvious why the suberyl chloride forms a coordination polymer: larger internal groups such as carbamates or ethers are perfectly capable of helicate assembly. In any case, as the reactive group was still intact, we attempted to perform a reaction on the aggregate, to see if it could be converted to a helicate complex. As it turned out, the metastable nature of the aggregate was important in controlling its reactivity. The reaction conditions were carefully chosen to minimize any disruption of the Fe-iminopyridine coordinations, which are sensitive to Cl^- and OH^- anions. By using silver salts, the chloride could be extruded from the ligand backbone, allowing water to perform an S_N1 reaction at the doubly benzylic carbocation center. Upon treatment with $AgClO_4$, the broad peaks for the aggregate in the ^1H NMR spectrum disappeared slowly, replaced by sharp peaks corresponding to a helicate cage (Figure 8b). No intermediates could be seen, just the final product, and reaction was complete after 20 h at 45 °C. The successful reaction was heartening, but upon closer inspection of the NMR spectrum, the product was not the expected suberol helicate **3** (i.e. the product of three S_n1 reactions at the ligand), but the *suberone* helicate **4**. This was surprising, to say the least, and created two questions: ***why*** did the ligand CHCl group get oxidized to a ketone, and ***how*** did it happen?

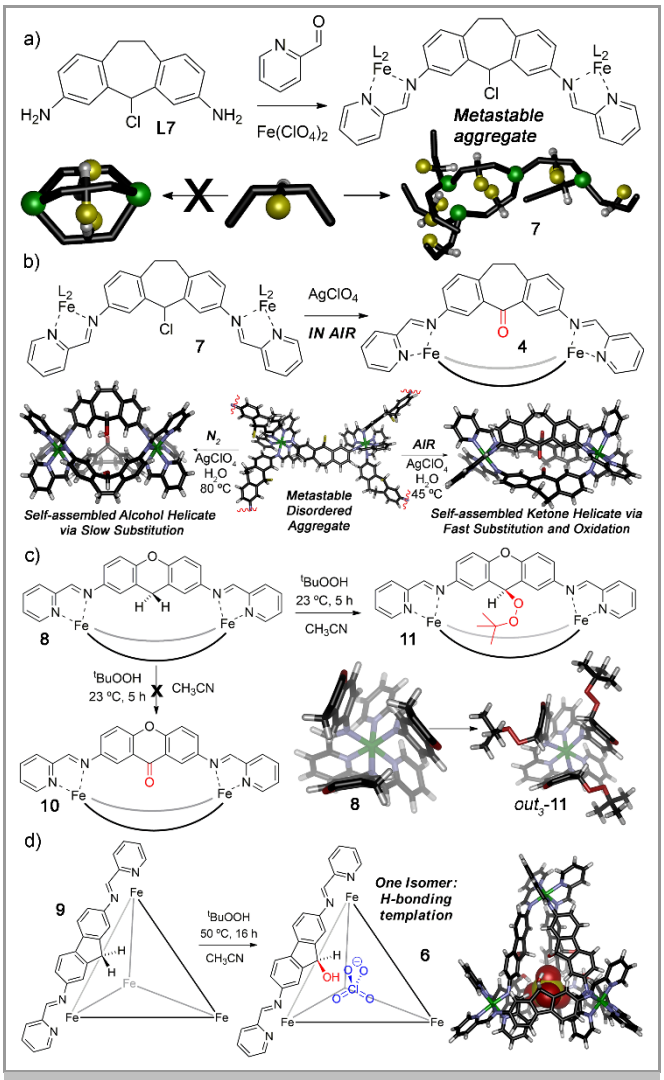

Figure 8. Post-assembly ligand oxidation. a) Formation of a meta-stable aggregate with ligand **L7**; b) post-assembly oxidative substitution of cage **7** and conversion to ketone-containing helicate **4**;[61] c) post-assembly oxidation of helicate **8** to peroxide **11**, as opposed to the expected carbonyl **10**;[62] d) diastereoselective oxidation of M_4L_6 cages.[62]

The "why" is relatively simple: we had previously shown that the suberone helicate **4** is far more stable than the suberol.[46] When the analogous reaction was performed on a non-assembled ligand equivalent, only the alcohol was formed *via* substitution.[61] The stability of the suberone helicate drives the reaction to the lowest energy product, diverting the outcome of a relatively simple reaction. The "how" is far more complex. The oxidation reaction requires air as the stoichiometric oxidant, and if performed under strictly air-free conditions, the substitution product is formed, far more slowly. But O_2 is not the active reagent in the process, and it quickly became clear that the Fe^{II} ions in the assembly play an important role in the ligand oxidation. As the assembly is reversible (and obviously changes throughout the reaction), a proportion of the Fe^{2+} ions are uncoordinated during the reaction, and evidently form Fe=O oxo species, which are catalytically active and can perform the ligand oxidation process. Strangely, the yield of the oxidation is high (>90 %), and the final product is an Fe^{II} complex, so any reactive iron salts are catalytic, or are reincorporated into the assembly after reaction.

As the starting material was just a broad mound in the NMR spectrum, the mechanism of this reaction was challenging to monitor, and no good evidence for the reactive Fe species was found. As such, we attempted to perform ligand oxidations on other self-assembled cages that were more defined in structure. The challenge was that the starting cage needed to be reactive, and less stable than the products, which was not immediately obvious. After some experimentation, we settled on diaminoxanthene **L8** and diaminofluorene **L9**. (Figure 8c,d).[62] Each of these ligands has activated methylene groups, and can be assembled into discrete cages **8** and **9** with Fe^{II} salts and PyCHO. The xanthene ligand forms a simple M_2L_3 helicate, but diaminofluorene is too linear to form an M_2L_3 assembly, so forms an M_4L_6 structure. Interestingly, this M_4L_6 cage **9** is far less stable than the fluorenol counterpart **6**, and forms as a mix of at least four different isomers, with both *mer* and *fac* centers at the vertices. Importantly, in each case, the corresponding ketone cage (xanthone or fluorenone) is ***less stable*** than the reactant. The xanthone complex **10** is strained (so much so that the Fe^{II} centers are slightly paramagnetic), and the fluorenone cannot take advantage of interligand H-bonds in the assembly (as can fluorenol **6**).

The two cages **8** and **9** were treated with a range of oxidants, including H_2O_2, benzoyl peroxide and $(^tBuO)_2$, unsuccessfully. However, when **8** was stirred with ^tBuOOH in CD_3CN, the reaction proceeded smoothly at room temperature in 5 h to give a new product. In this case, the reaction product was not the ketone **10**, but the ^{t}butyl peroxide **11** (Figure 8c). The reaction occurred diastereoselectively, and only one isomer (*out*$_3$, presumably due to sterics) was seen. The reaction was monitored by NMR, and the buildup and loss of the mono- and bis- intermediate products could be seen over time. The fluorene cage **9** could also be oxidized with ^tBuOOH: in this case, selective oxidation required the presence of a ClO_4^- ion as template, and formed the fluorenol cage **6** in excellent yield after warming at 50 °C. The reaction was again stereoselective, and only one isomer of **6** was formed, due to the favorable H-bonding in the product.

These outcomes follow the same pattern as the suberyl chloride oxidation. When the uncomplexed ligands were oxidized by Fe^{II} salts and ^tBuOOH, the reaction was much more sluggish and the ***ketone*** products were formed.[62] Most CH oxidation reactions of secondary CH_2 groups yield the ketones, but when the reaction occurs on self-assembled cages, the outcome is deviated to favor the most stable assembly, either the fluorenol cage, or the xanthyl peroxide helicate. Again, the question of "why" and "how" arise. The fluorene cage **9** oxidation outcome is obvious, as the hexa-ol **6** is most stable.[45] The xanthene cage **8** oxidation is unusual: the ketone product is highly strained, so is not a favorable product, but the corresponding alcohol (xanthol) is not formed, which would be the logical alternative. We attempted to independently synthesize the self-assembly cage complex with 2,7-diaminoxanthol with limited success: it appears to form a mixture of M_4L_6 cage isomers, and fragmented easily under ESI-MS conditions.[62] Whatever the reason, it appears that the *tert*-butylperoxide helicate **11** is the most stable target; hence, it is the observed product. As for the "how", it is clear that even though these self-assembled cages are highly stable, small amounts of uncomplexed Fe^{II} ions are present in solution, leached from the cages. The concentration is small, but they are capable of catalyzing oxidation reactions in the presence of suitable stoichiometric reagents. If the products are favorable, highly efficient ligand oxidation is possible with ***no*** accompanying oxidation of the metal centers. In essence, the cages provide the catalysts for their own transformation, and direct the reactions to the most stable self-assembled product, independent of the "usual" reaction products.

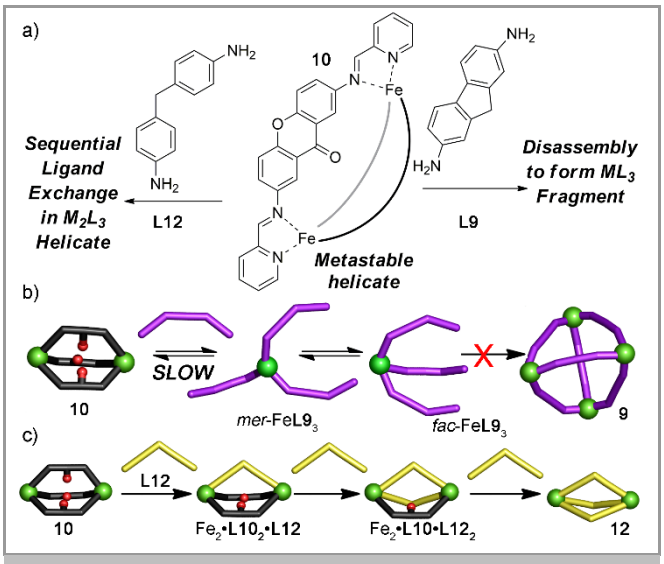

Figure 8. a) Variable subcomponent exchange depending on ligand rigidity; b) cage **10** is converted to FeL_3 fragments when reacted with ligand **L9**; c) the same cage undergoes iterative ligand replacement reactions with ligand **L12**.[63]

The reactivity of metastable assemblies led to a question: can we "switch" the structure of a cage complex into another type of assembly motif *via* subcomponent exchange? The ultimate goal would be to perform a switching process that ostensibly goes against thermodynamics, i.e. switching from a small M_2L_3 helicate (which is entropically and often enthalpically, favored) to a larger M_4L_6 tetrahedron. The stoichiometry of assembly is identical, so it should be possible: the challenge is to overcome the thermodynamic unfavorability of the M_4L_6 assembly. Our "solution" didn't actually end up being a solution, but it's an interesting idea: can we use a metastable helicate such as the

xanthone cage **10** as starting material?[63] Adding diamine ligands to **10** showed some extremely unusual self-assembly behavior. Depending on the nature of diamine, multiple different reaction outcomes could be observed that were independent of the nucleophilicity of the diamine, and were instead completely dominated by the stability of the assembly. Varying diamine ligands gave products as different as ML_3 "fragments", mixed heterocomplexes or rapid formation of M_2L_3 helicates, and the reaction times varied from <2 mins at 23 °C to multiple days heating. The various outcomes are far too many to be described here, but the reader is directed to ref. 63 for a full account, with apologies for its length. One quick illustration of the large differences in reactivity between highly similar ligands is shown in Figure 9.

Diamino-diphenylmethane (**L12**) and diaminofluorene (**L9**) vary only in rigidity and coordination angle: they are exactly as reactive as each other towards small molecule electrophiles. However, their behaviors when added to the metastable helicate **10** are quite different. **L12** has approximately the same length and coordination angle as diaminoxanthene, so that ligand simply displaces the xanthone ligands from the helicate one by one (Figure 9c). This can be monitored by ^{1}H NMR and the intermediates observed throughout the reaction. Diaminofluorene **L9** is not a good ligand for assembly, as the M_4L_6 cage is strained and exists as multiple isomers.[62] Usually in subcomponent exchange, when a diamine forms a less stable cage than the starting material, no reaction occurs and the other diamine just hangs around in the solution.[46,64] In this case, however, the reaction is very quick, and the xanthone helicate is displaced in 2 h at 23 °C. The product is not a cage, but a simple ML_3 fragment: opening the helicate is so easy that a new assembly is not necessary. This is just a quick taste of the various tests that we did in this study, and many of these reactivity differences are quite difficult to explain. As for the original idea of switching between different cage stoichiometries, we're still trying…

V. Molecular Recognition and Catalysis

As interesting and fun as these studies were, they didn't actually solve the major challenge, which was to create an enzyme-mimicking host molecule with internalized functions. We had shown that functional groups can have a wide range of effects on cage assembly and reactivity, but all the assemblies were too small to act as hosts for anything bigger than a perchlorate anion. The next step was to take the diaminofluorene scaffold, which successfully formed M_4L_6 assemblies with internalized functional groups,[55,56,62] and simply make the cage bigger by making the ligands longer. This was not necessarily a good idea: by lengthening the ligand, the assembly will be larger, but the "gaps" between the ligands is also larger. There are many, many examples of large superstructures with large spaces between the ligands,[65] and beautiful though they may be, they are often ineffective at binding small molecule guests, because the molecules can freely diffuse in and out of the cavity. Biomimetic catalysis requires that the host bind the guests for a defined period of time,[1,34b] so they can be activated and transformed. Having said that, the cages formed by short ligands couldn't perform reactions either, so we decided to test it out anyway.

Extending the ligand scaffold was simple: 2,7-dibromofluorene can be easily reacted with N-Boc-aminophenylboronic acid, as can an equivalent with two CH_2CO_2Et groups at the fluorenyl center.[66] Deprotection (and ester hydrolysis, if necessary) gives extended diamine ligands **L13** and **L14**, which can be reacted with 2-formylpyridine and Fe^{II} salts to give M_4L_6 tetrahedral cages **13** and **14**. The extended fluorene scaffold behaves differently to the shorter version **L6** upon assembly, despite displaying identical coordination angles and geometries. Whereas **6** formed a single *mer₃fac* M_4L_6 complex upon assembly,[56] **13** and **14** all form the "standard" *fac₄* M_4L_6 tetrahedral structures that have been extensively studied by Nitschke.[42] As expected, these long ligands do not allow stereocontrol at the *fac* Fe centers, and mixtures of tetrahedral isomers with S_4, C_3 and T symmetry are observed (Figure 10). The isomer ratios depend on the internal functional groups: fluorene cage **13** is formed as a 41:48:11 mixture of S_4, C_3 and T isomers, whereas acid cage **14** only forms the S_4 and C_3 isomers (55:45 ratio).[66]

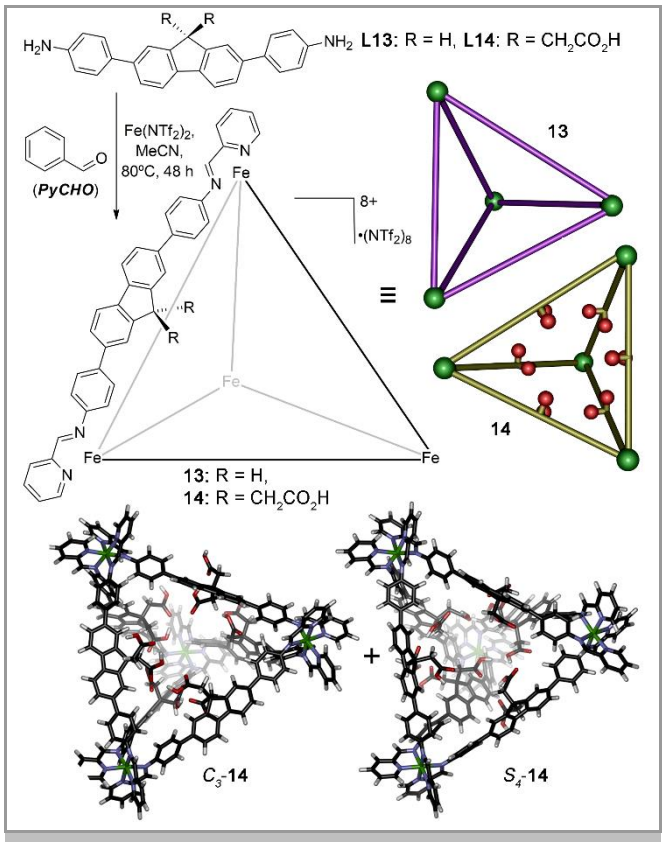

Figure 10. A host cage internally functionalized with acidic residues.

Having formed a cage with internalized functional groups, the next question was to determine what it could do. Choice of reaction was not trivial - there are numerous limitations in reactions, mainly due to the tolerance of reactive species by the cage itself. As such, we tested a simple process first, mainly to see how effective an acid catalyst the cage was, and what conditions it was tolerant to.[66] Benzaldehyde dimethyl acetal (**BDA**, Figure 11a) was added to a solution of CD_3CN with 4 mol% cage **14** and a small excess of water, then stirred and the solvolysis reaction monitored. As a control, the reaction was repeated with 24% acid ligand **L15** (which corresponds to the same concentration of acidic groups, just not self-assembled). The initial rate of solvolysis was 1070-fold faster with the cage complex than the control ligand, and reaction was complete in ~ 2h at room

temperature. The cage structure was maintained throughout the reaction, and no trans-imination was observed with the aldehyde product. Electron-withdrawn acetals (e.g. 2-formylpyridine dimethylacetal, **FPA**) reacted more slowly, requiring refluxing conditions, but the reaction still went to completion. Importantly, the cage **14** was tolerant to the reaction conditions for >24 h at reflux.

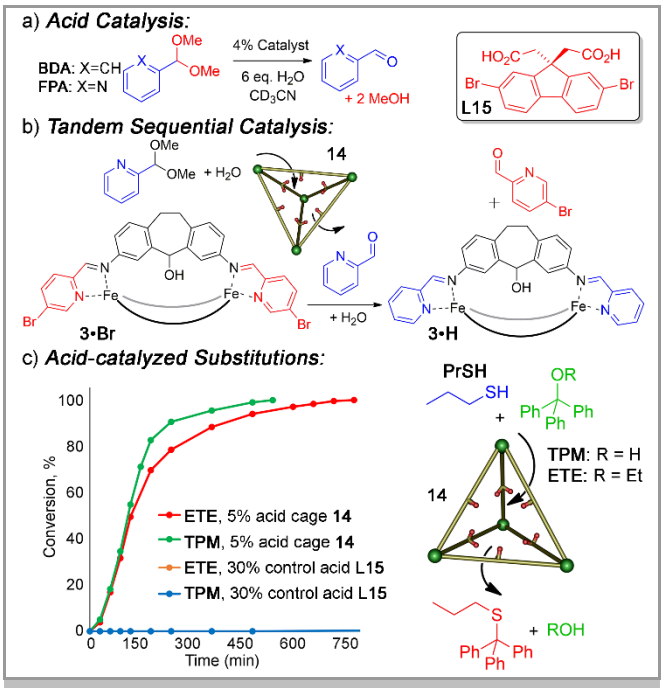

Figure 11. Reactions catalyzed by acid cage 14. a) Accelerated acetal solvolysis; b) sequential tandem catalysis of both acetal deprotection and helicate subcomponent exchange;[66] c) accelerated trityl etherification.[69]

This illustrated the reactivity of the cage, but an acetal deprotection isn't particularly interesting. The deprotection of the pyridyl acetal introduced a more interesting application, however: can the cage catalyze a cage-to-cage transformation? The brominated helicate **3•Br** can be converted to the pyridyl counterpart **3•H** by treatment with PyCHO and water, but it requires heating.[52] If PyCHO was protected as the acetal, a tandem deprotection/subcomponent exchange process is possible (Figure 11b). This is an excellent showcase for the acid cage, because it is a highly effective, yet ***mild*** acid catalyst. This combination of mild reactions and high activity was essential for success. When 4% cage **14** was heated with **FPA**, a small amount of water, and brominated helicate **3•Br** in CD_3CN, the deprotection reaction proceeded smoothly.[66] After a small delay, the resulting deprotected PyCHO displaced BrPyCHO from the helicate. Reaction was complete after 8 h, and minimal decomposition of the cage was observed: all that was left at the end of the reaction was suberol helicate **3**, BrPyCHO and methanol. In contrast, when the reaction was performed with control acid **L15**, no deprotection occurred, as the acid was not a competent catalyst. If the reaction was performed with CF_3COOH, deprotection was possible, but the small molecule acid was incompatible with the helicate, and decomposition rather than trans-imination occurred. Only with the mild, yet reactive cage **14** did the tandem process work successfully.

Accelerating a reaction in a cage was an important first step, but simple rate accelerations are not the real goal here. Any catalyst can accelerate a reaction; why would we need such a complex catalyst to do that? Enzymes exert far greater control on their reactions, not just simply accelerating them. The key is molecular recognition – by binding multiple substrates, size-based selectivity as well as enantioselectivity is possible. One other facet that is often overlooked is that enzymes can change the mechanism of a reaction.[67] A common example is general acid-base catalysis,[68] whereby sidechains such as histidine deprotonate the nucleophile (usually water), directly involving themselves in the rate equation.

While investigating the scope of reactions that cage **14** can catalyze, we stumbled across an interesting example of that kind of effect. The reaction, again, was quite simple: the acid-catalyzed thioetherification of activated alcohols such as triphenylmethanol. (Figure 11c).[69] Cage **14** is an excellent catalyst for that process too, and shows a 1000-fold acceleration of the reaction between **TPM** and *n*-propanethiol (**PrSH**). Surprisingly, the cage is tolerant to the thiols, even at elevated temperature. The rate acceleration is not the interesting part of this process, though. Nucleophilic substitution at trityl centers is perhaps the most "S_N1-like" of all S_N1 reactions: the highly stable cation and large amount of steric hindrance make concerted substitution essentially impossible. As such, the rate of the reaction should be independent of the type (within reason) and concentration of nucleophile. This is true for simple, small molecule acid catalysts: when CF_3COOH was used as catalyst (Figure 12c), no dependence on nucleophile concentration was seen. However, the initial rate of the reaction with 4% acid cage varied significantly with different nucleophiles: cyclohexanethiol and ethanol were both suitable substrates and gave good conversions to product, but reacted far more slowly. In addition, the rate of the reaction was dependent on the *concentration* of **PrSH** (Figure 12b), which was extremely surprising. Even more surprising was that the same reaction using ethyl tritylether as electrophile showed *no dependence* on nucleophile concentration, despite the reactivity being essentially identical to that of **TPM** (Figure 11c). This suggests that *molecular recognition* plays a part in the reaction. The acid cage is not a "usual" host, in that it has large gaps between the walls that allow rapid ingress and egress of substrates. The exchange rate is fast on the NMR timescale, so no long-lived Michaelis complexes can be observed, but the affinity can be analyzed by UV-Vis titrations. These show that a wide range of neutral species, including alkanethiols, **TPM**, and derivatives show binding affinities K_a up to ~ 10^5 M^{-1} in CH_3CN. Most importantly, the cavity size is large enough to bind multiple guests at once, and by fitting the UV titration data to multiple different binding models,[70] it became clear that **PrSH** and **CySH** were most favorably bound in a 2:1 manner. The rapid ingress/egress of guests also allows the cage to act as a catalyst. While the equilibrium constants of binding are high, the fast in/out exchange of the various components allows turnover, essential for effective reaction.

This binding affinity analysis led to the postulated mechanism in Figure 12a, which theoretically explains the differing rate profiles observed. Either the nucleophile and/or the electrophile can bind in the cavity of **14**, followed by a second equilibrium event to form a heteroternary complex. If the electrophile (e.g. **ETE**) is activated before the nucleophile also binds, it can be ejected from the catalyst and reacts in free solution with nucleophile, leading

to an "S_N1"-type reaction. If, however, the electrophile is activated in the ternary complex (e.g. **TPM**), [Nu] is part of the rate determining step, and so nucleophile dependence is seen. Exactly why **ETE** and **TPM** show such differences is unclear, but one possibility is that **ETE** is larger, and doesn't favor a ternary complex.

Other important observations from this process are that the reaction can suffer from substrate inhibition, a common problem with enzymatic catalysis. If a large excess (15 mol.-eq.) of **PrSH** is added, it saturates the cage catalyst, preventing reaction. Interestingly, product inhibition was not observed. This is far more common in synthetic host-based catalysis, especially for dimerization reactions where binding a single product molecule is more entropically favorable than binding two reactants. In this case, propyl tritylsulfide product has a 10-fold lower affinity for **14** than does **TPM**, so product inhibition is not observed.

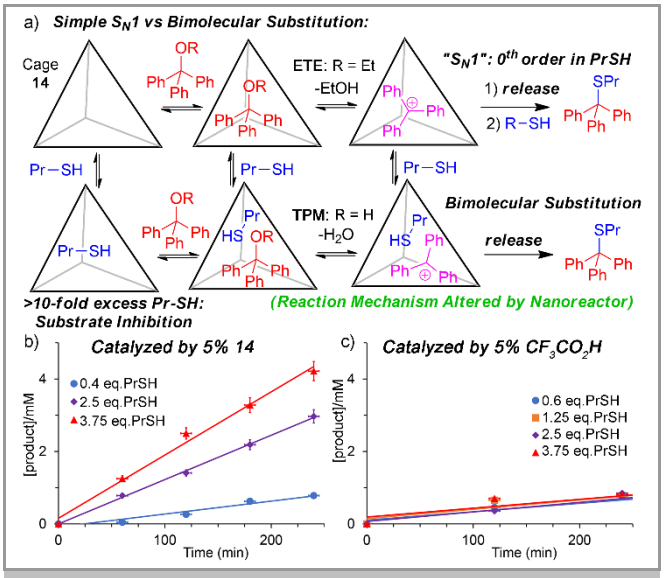

Figure 12. Acid cage 14 alters the prevailing mechanism of cavity-based reactions. a) Proposed host:guest catalysis in thioetherification reactions; b) rate of the cage-catalyzed S_N1 process is dependent on [nucleophile], as opposed to the rate of the process catalyzed by c) simple small molecule acids.[69]

There was one more little wrinkle to this reaction. As the electrophile is activated by acid, more basic leaving groups react faster. When *N*-trityltoluidine was used as electrophile, the trityl group was activated in minutes at room temperature. Of course, the byproduct of this was toluidine, which could be used as an "OFF" logic gate, because the product of the reactions destroys the catalyst in a self-immolative process.[69] This had limited utility, as the cage was destroyed in the process, but it was interesting that 25% of the starting material could be reacted by 5% cage before the catalyst was consumed.

The acid cage **14** has a variety of uses, and we are currently investigating other reactions that proceed via oxocarbenium intermediates. Obviously, this molecule fits the "goal" of the project, in that we have created a functionalized, enzyme-mimicking active site, but it turns out that the simple unfunctionalized fluorenyl cage **13** can contribute to the project as well. While we were performing all the necessary control reactions to ensure that cage **14** was the active catalyst, we came across an unusual observation. Cage **13** cannot promote the thioetherification reaction by itself at all, and the acid ligand **L15** is an extremely poor catalyst, but when they are combined, significant reactivity was observed (Figure 13a).[71] It's getting repetitive to say that this was surprising at this point, but this system is the gift that keeps on giving.

As shown in Figure 12b, the reaction of **TPM** with **PrSH** when catalyzed by 5% **13**/30% **L15** occurs at ~25% the rate of the reaction catalyzed by acid cage **14**, which is still a 50-fold increase over that of **L15**. Again, the question is why? The acid ligand must be acting as a "cofactor",[72] forming a host:guest complex (the "holoenzyme") with cage **13** (the "apoenzyme") that can catalyze the reaction. This is extremely unusual in synthetic receptors, as it requires the formation of ternary (or higher) host:guest complexes. This is obviously entropically unfavorable, and generally only occurs in large superstructures[17] or with small cofactors like solvated H^+ or OH^- ions.[73,74]

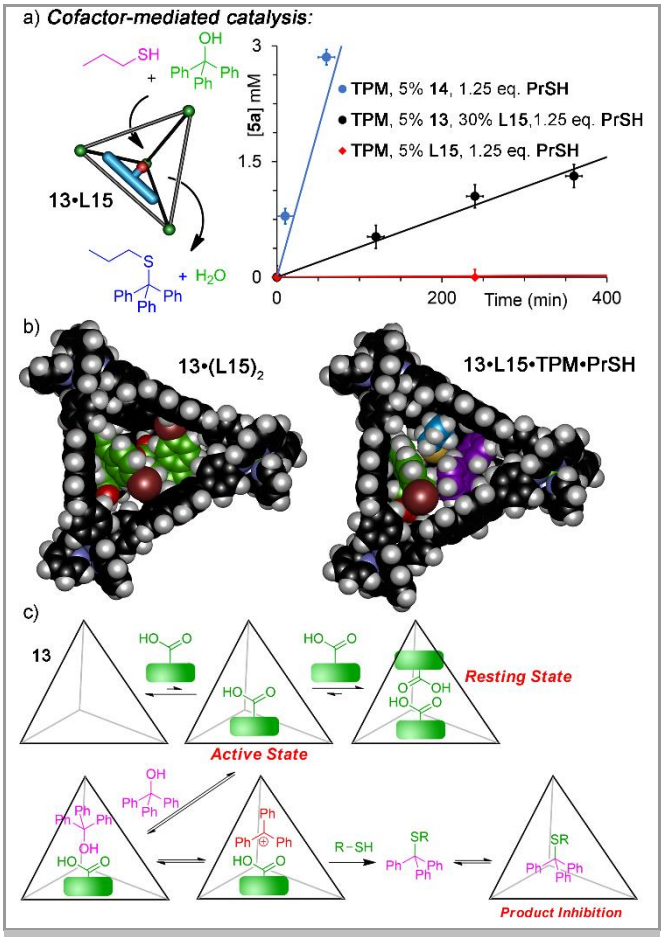

Figure 13. Cofactor-mediated catalysis. a) Combination of unfunctionalized cage **13** and acid ligand **L15** accelerates thioetherification reactions; b) molecular models of the host:guest complex between cage **13** and two molecules of **L15**, and the complex between **13**, **L15**, electrophile **TPM**, and nucleophile **PrSH**; c) host:guest processes present in the cofactor-mediated reaction.[71]

This necessitated an investigation into the host:guest properties of **13**. Molecular models of **13** binding the various components of the cofactor-mediated reaction are shown in Figure 13b, and they show that there is enough space in the host to bind multiple guests at once, even relatively large species such as **L15** and **TPM**. Of course, this does not mean that it actually happens, merely that there is enough space to do so. UV/Vis titrations and binding

isotherm analysis of a series of acid catalysts, thiol nucleophiles and trityl electrophiles showed that binding constants were high (up to K_a = 10^5 M^{-1} for naphthoic acid[71]), with fast in/out exchange as before. While definitive proof for 2:1 complexes vs. 1:1 complexes is often challenging, three guests showed affinity for the cage in a 2:1 manner with greater than *p* values below 0.001: **ETE**, *n*-octanethiol, and control acid **L15**. In the case of **L15**, the binding was highly cooperative (α ($4K_2/K_1$) = 51), presumably due to favorable H-bonding in the cage.[71]

The reaction rate was highly variable, depending on the nature of the cofactor and electrophile. Different acid cofactors of essentially identical pK_a (e.g. benzoic acid, naphthoic acid, anthroic acid) gave reaction rates that varied by up to 4-fold, depending on the binding in the host. The most interesting behavior was shown by the combination of **13•L15** and **TPM**. In this case, the reaction rate was again dependent on [Nu], despite the fact that this is still an S_N1 reaction, but was *independent* of [**L15**]. The mechanism is illustrated in Figure 13c, and relies on the small concentration of the "active" 1:1 complex **13•L15** favoring the binding of the **TPM** electrophile, although there is still much that is unclear about this process. The other acid cofactors and trityl electrophiles did not show this dependence, and generally showed classical S_N1 rate profiles that were dependent on the concentration of cofactor. Interestingly, the cofactor-mediated processes were affected somewhat by product inhibition, as propyl trityl sulfide was a good guest for the unfunctionalized cage, but did not show any appreciable substrate inhibition, as was shown by acid cage **14**. Small changes to the structure of the cage can have large effects on the relative affinity of different guests.

VI. Conclusions and Outlook

Well, it only took 10 years, but we did manage to create a self-assembled host molecule that has internal functions, an "active site", and can perform enzyme-like catalysis of reactions. Along the way, there were numerous diversions into self-sorting, self-assembly mechanisms and post-assembly reactivity, but as with all research, the journey is the point, not necessarily the destination. Having said that, we have reached "a" destination, not "the" destination. Yes, we have created a biomimetic cage complex, but we have only just scratched the surface. Cage **14** is well-suited to catalyse reactions that proceed *via* stabilized carbocations, notably oxocarbenium ions, so more complex multi-step reactions can be envisaged. In addition, other functionalities can be incorporated into the scaffold, such as basic groups or even amphiphilic systems that have both acid and basic functions at the same time. Incorporation of basic groups is more challenging, mainly due to incompatibility with the Fe-iminopyridine centers, but we are confident it can be done.

Of course, there are many, many more applications out there, some that are far more difficult. Obviously, true enzyme mimics need to function in water, which is not simple. Nitschke has shown an exhaustively researched roadmap for solubilisation of M-iminopyridine cages in water,[40] but how that affects functionalized cages is unknown. In addition, size-based substrate selectivity, enantioselectivity and sequestration of incompatible reactants for concurrent tandem catalysis are all possible targets for catalysis, so there is plenty of work to keep us busy.

Funding Information

RJH would like to thank the National Science Foundation (CHE-1151773 and 1708019) for funding of all these projects, as well as the UC Riverside Center for Catalysis.

Acknowledgment

I would like to thank all the students who have worked in my lab over the years, notably Amber Johnson, Michael Young, Lauren Holloway, Paul Bogie, Tabitha Miller and Courtney Ngai, who performed the bulk of the work described here. I would also like to thank Prof. Julius Rebek, Jr. for setting me on this path, and Prof. Jonathan Nitschke for providing a rapidly moving target to follow.

References

(1) Hof, F.; Craig, S. L.; Nuckolls, C.; Rebek, J., Jr. *Angew. Chem., Int. Ed.* **2002**, *41*, 1488.
(2) Diederich, F. *Angew. Chem., Int. Ed. Engl.* **1988**, *27*, 362.
(3) Murakami, Y.; Kikuchi, J.-I.; Hisaeda, Y.; Hayashida, O. *Chem. Rev.* **1996**, 96, 721
(4) Breslow, R. *Acc. Chem. Res.* **1995**, *28*, 146–153.
(5) Cram, D. J. *Angew. Chem., Int. Ed. Engl.* **1988**, *27*, 1009.
(6) Kang, J. M.; Rebek, J., Jr. *Nature* **1997**, *385*, 50.
(7) Jordan, J. H.; Gibb, B. C. *Chem. Soc. Rev.* **2015**, *44*, 547.
(8) Hooley, R. J.; Rebek, J., Jr. *Chem. Biol.* **2009**, *16*, 255.
(9) Gissot, A.; Rebek, J., Jr. *J. Am. Chem. Soc.* **2004**, *126*, 7424.
(10) Hooley, R.J.; Restorp, P.; Iwasawa, T.; Rebek, J., Jr. *J. Am. Chem. Soc.*, **2007**, *129*, 15639.
(11) Hooley, R.J.; Iwasawa, T.; Rebek, J., Jr. *J. Am. Chem. Soc.* **2007**, *129*, 15330.
(12) (a) Caulder, D. L.; Raymond, K. N. *Acc. Chem. Res.* **1999**, *32*, 975. (b) Caulder, D. L.; Brückner, C.; Powers, R. E.; König, S.; Parac, T. N.; Leary, J. A.; Raymond, K. N. *J. Am. Chem. Soc.* **2001**, *123*, 8923.
(13) (a) Fujita, M.; Tominaga, M.; Hori, A.; Therrien, B. *Acc. Chem. Res.* **2005**, *38*, 371. (b) Fujita, M.; Umemoto, K.; Yoshizawa, M.; Fujita, N.; Kusukawa, T.; Biradha, K. *Chem. Commun.* **2001**, 509.
(14) (a) Sato, S.; Ishido, Y.; Fujita, M. *J. Am. Chem. Soc.* **2009**, 131, 6064. (b) Suzuki, K; Kawano, M.; Sato, S.; Fujita, M. *J. Am. Chem. Soc.* **2007**, 129, 10652–10653. (c) Fujita, D.; Suzuki, K.; Sato, S.; Yagi-Utsumi, M.; Yamaguchi, Y.; Mizuno, N.; Kumasaka, T.; Takata, M.; Noda, M.; Uchiyama, S.; Kato, K.; Fujita, M. *Nat. Commun.* **2012**, *3*, 2093. (d) Sun, Q.-F.; Murase, T.; Sato, S.; Fujita, M. *Angew. Chem. Int. Ed.*, **2011**, *50*, 10318.
(15) (a) Sato, S.; Iida, J; Suzuki, K; Kawano, M.; Ozeki, T.; Fujita, M. *Science* **2006**, *313*, 1273. (b) Suzuki, K; Iida, J; Sato, S, Kawano, M.; Fujita, M. *Angew. Chem., Int. Ed.* **2008**, *47*, 5780.
(16) (a) Yoshizawa, M.; Tamura, M.; Fujita, M. *Science* **2006**, *312*, 251. (b) Ueda, Y.; Ito, H.; Fujita, D.; Fujita, M. *J. Am. Chem. Soc.* **2017**, *139*, 6090.
(17) Wang, Q. -Q.; Gonell, S.; Leenders, S. H. A. M.; Dürr, M.; Ivanović-Burmazović, I.; Reek, J. N. H. *Nat. Chem.* **2016**, *8*, 225.
(18) Bolliger, J. L.; Belenguer, A. M.; Nitschke, J. R. *Angew. Chem., Int. Ed.*, **2013**, *52*, 7958.
(19) Yue, N.L.S.; Eisler, D.J.; Jennings, M.C.; Puddephatt, R.J. *Inorg. Chem.* **2004**, *43*, 7671.
(20) (a) Lewis, J. E. M.; Gavey, E. L.; Cameron, S. A.; Crowley, J. D. *Chem. Sci.*, **2012**, *3*, 778. (b) Preston, D.; Lewis, J. E. M.; Crowley, J. D. *J. Am. Chem. Soc.*, **2017**, *139*, 2379.
(21) Clever, G. H.; Punt, P. *Acc. Chem. Res.*, **2017**, *50*, 2233.
(22) Liao, P.; Langloss, B.W.; Johnson, A.M.; Knudsen, E.R.; Tham, F.S.; Julian, R.R.; Hooley, R.J. *Chem. Commun.* **2010**, *46*, 4932.
(23) Martí-Centelles, V.; Lawrence, A. L.; Lusby, P. J. *J. Am. Chem. Soc.* **2018**, *140*, 2862.
(24) Johnson, A.M.; Moshe, O.; Gamboa, A.S.; Langloss, B.W.; Limtiaco, J.F.K.; Larive, C.K.; Hooley, R.J. *Inorg. Chem.* **2011**, *50*, 9430.
(25) Johnson, A.M.; Hooley, R.J. *Inorg. Chem.,* **2011**, *50*, 4671.
(26) Young, T.A.; Martí-Centelles, V.; Wang, J.; Lusby, P.J.; Duarte, F. *J. Am. Chem. Soc.* **2020**, *142*, 1300.

(27) August, D.P.; Nichol, G.S.; Lusby, P.J. *Angew. Chem. Int. Ed.*, 2012, **55**, 15022.

(28) (a) Freye, S.; Hey, J.; Torras-Galán, A.; Stalke, D.; Herbst-Irmer, R.; John, M.; Clever, G. H. *Angew. Chem. Int. Ed.*, **2012**, *51*, 2191. (b) Frank, M.; Ahrens, J.; Bejenke, I.; Krick, M.; Schwarzer, D.; Clever, G. H. *J. Am. Chem. Soc.*, **2016**, *138*, 8279.

(29) Johnson, A.M.; Young, M.C.; Zhang, X.; Julian, R.R.; Hooley, R.J. *J. Am. Chem. Soc.* **2013**, *135*, 17723.

(30) Johnson, A.M.; Wiley, C.A.; Young, M.C.; Zhang, X.; Lyon, Y.; Julian, R.R.; Hooley, R.J. *Angew. Chem. Int. Ed.* **2015**, *54*, 5641.

(31) Liu, C.-L.; Zhang, R.-L. Lin, C.-S.; Zhou, L.-P.; Cai, L,-X.; Kong, J.-T.; Yang, S.-Q.; Han, K.-L.; Sun, Q.-F. *J. Am. Chem. Soc.* **2017**, *139*, 12474.

(32) (a) Jing, X.; He, C.; Zhao, L.; Duan, C. *Acc. Chem. Res.* **2019**, *52*, 100. (b) Li, X.-Z.; Zhou, L.-P.; Yan, L.-L.; Yuan, D.-Q.; Lin, C.-S.; Sun, Q.-F. *J. Am. Chem. Soc.* **2017**, *139*, 8237.

(33) Jing, X.; He, C.; Yang, Y.; Duan, C. *J. Am. Chem. Soc.* **2017**, *139*, 3967.

(34) (a) Hong, C. M.; Bergman, R. G.; Raymond, K. N.; Toste, F. D. *Acc. Chem. Res.* **2018**, *51*, 2447. (b) Brown, C. J.; Toste, F. D.; Bergman, R. G.; Raymond, K. N. *Chem. Rev.* **2015**, *115*, 3012.

(35) Smulders, M. M. J.; Riddell, I. A.; Browne, C.; Nitschke, J. R. *Chem. Soc. Rev.* **2013**, *42*, 1728.

(36) Hannon, M. J.; Painting, C. L.; Jackson, A.; Hamblin, J.; Errington, W. *Chem. Commun.*, **1997**, 1807.

(37) McConnell, A. J.; Wood, C. S.; Neelakandan, P. P.; Nitschke, J. R. *Chem. Rev.* **2015**, *115*, 7729.

(38) Mal, P.; Schultz, D; Beyeh, K.; Rissanen, K.; Nitschke, J. R. *Angew. Chem., Int. Ed.* **2008**, *47*, 8297.

(39) Bilbeisi, R. A.; Clegg, J. K.; Elgrishi, N.; de Hatten, X.; Devillard, M.; Breiner, B.; Mal, P.; Nitschke, J. R. *J. Am. Chem. Soc.* **2012**, *134*, 5110.

(40) Percástegui, E. G.; Mosquera, J.; Ronson, T. K.; Plajer, A. J.; Kieffer, M.; Nitschke, J. R. *Chem. Sci.* **2019**, *10*, 2006.

(41) Castilla, A. M.; Miller, M. A.; Nitschke, J. R.; Smulders, M. M. J. *Angew. Chem. Int. Ed.* **2016**, *55*, 10616.

(42) (a) Meng, W.; Clegg, J. K.; Thoburn, J. D.; Nitschke, J. R. *J. Am. Chem. Soc.* **2011**, *133*, 13652. (b) Ronson, T. K.; Meng, W.; Nitschke, J. R. *J. Am. Chem. Soc.* **2017**, *139*, 9698.

(43) Kieffer, M.; Pilgrim, B. S.; Ronson, T. K.; Roberts, D. A.; Aleksanyan, M.; Nitschke, J. R. *J. Am. Chem. Soc.* **2016**, *138*, 6813.

(44) Young, M.C.; Johnson, A.M.; Gamboa, A.S.; Hooley, R.J. *Chem. Commun.* **2013**, *49,* 1627.

(45) Young, M.C.; Johnson, A.M.; Hooley, R.J. *Chem. Commun.* **2014**, *50*, 1378.

(46) Holloway, L.R.; Young, M.C.; Beran, G.J.O.; Hooley, R.J. *Chem. Sci.* **2015**, *6*, 4801.

(47) Wu, A.; Isaacs, L. *J. Am. Chem. Soc.* **2003**, *125*, 4831.

(48) Persch, E.; Dumele, O.; Diederich; F. *Angew. Chem. Int. Ed.* **2015**, *54*, 3290.

(49) (a) Mukhopadhyay, P.; Wu, A.; Isaacs, L. *J. Org. Chem.* **2004**, *69*, 6157. (b) Yamanaka, M.; Yamada, Y.; Sei, Y.; Yamaguchi, K.; Kobayashi, K. *J. Am. Chem. Soc.* **2006**, *128*, 1531.

(50) (a) Sun, Q.-F.; Sato, S.; Fujita, M. *Angew. Chem. Int Ed.* **2014**, *53*, 13510. (b) Saha, M.L.; Schmittel, M. *J. Am. Chem. Soc.* **2013**, *135*, 17743. (c) Smulders, M. M. J.; Jiménez, A.; Nitschke, J. R. *Angew. Chem., Int. Ed.* **2012**, *51*, 6681. (d) Saha, M. L.; Pramanik, S.; Schmittel, M. *Chem. Commun.* **2012**, *48*, 9459.

(51) (a) Hristova, Y. R.; Smulders, M. M. J.; Clegg, J. K.; Breiner, B.; Nitschke, J. R. *Chem. Sci.* **2011**, *2*, 638. (b) Wood, C. S.; Ronson, T. K.; Belenguer, A. M.; Holstein, J. J.; Nitschke, J. R. *Nat. Chem.* **2015**, *7*, 354. (c) Neelakandan, P. P.; Jiménez, A.; Thoburn, J. D.; Nitschke, J. R. *Angew. Chem., Int. Ed.* **2015**, *54*, 14378.

(52) Wiley, C.A.; Holloway, L.R.; Miller, T.F.; Lyon, Y.; Julian, R.R.; Hooley, R.J. *Inorg. Chem.* **2016,** *55*, 9805.

(53) McConnell, A.J.; Aitchison, C. M.; Grommet, A. B.; Nitschke, J. R. *J. Am. Chem. Soc.* **2017**, *139*, 6294-6297.

(54) (a) McConnell, A.J. *Supramol. Chem.* **2018**, *30*, 858-868. (b) Bilbeisi, R. A.; Zarra, S.; Feltham, H. L. C.; Jameson, G. N. L.; Clegg, J. K.; Brooker, S.; Nitschke, J. R. *Chem. - Eur. J.* **2013**, *19*, 8058-8062.

(55) Miller, T.F.; Holloway, L.R.; Nye, P.P.; Lyon, Y.; Beran, G.J.O.; Harman, W.H.; Julian, R.R.; Hooley, R.J. *Inorg. Chem.* **2018**, *57,* 13386.

(56) Young, M.C.; Holloway, L.R.; Johnson, A.M.; Hooley, R.J. *Angew. Chem. Int. Ed.* **2014**, *53*, 9832.

(57) Tanabe, K. K.; Cohen, S. M. *Chem. Soc. Rev.*, **2011**, *40*, 498.

(58) Roberts, D. A.; Pilgrim, B.S.; Cooper, J.D.; Ronson, T.K.; Zarra, S.; Nitschke, J. R. *J. Am. Chem. Soc.* **2015**, *137*, 10068.

(59) Ronson, T.K.; Pilgrim, B.S.; Nitschke, J. R. *J. Am. Chem. Soc.* **2016**, *138*, 10417.

(60) Roberts, D. A.; Pilgrim, B.S.; Sirvinskaite, G.; Ronson, T.K.; Nitschke, J. R. *J. Am. Chem. Soc.* **2018**, *140*, 9616.

(61) Holloway, L.R.; McGarraugh, H.H.; Young, M.C.; Sontising, W.; Beran, G.J.O.; Hooley, R.J. *Chem. Sci.* **2016**, *7*, 4423.

(62) Holloway, L.R.; Bogie, P.M.; Lyon, Y.; Julian, R.R.; Hooley, R.J. *Inorg. Chem.* **2017**, *56*, 11435.

(63) Bogie, P.M.; Holloway, L.R.; Lyon, Y.; Onishi, N.C.; Beran, G.J.O.; Julian, R.R.; Hooley, R.J. *Inorg. Chem.* **2018**, *57*, 4155.

(64) Roberts, D. A.; Castilla, A.M.; Ronson, T.K.; Nitschke, J. R. *J. Am. Chem. Soc.* **2014**, *136*, 8201.

(65) Chakrabarty, R.; Mukherjee, P. S.; Stang, P. J. *Chem. Rev.* **2011**, *11*, 6810.

(66) Holloway, L.R.; Bogie, P.M.; Lyon, Y.; Ngai, C.; Miller, T.F.; Julian, R.R.; Hooley, R.J. *J. Am. Chem. Soc.* **2018**, *140,* 8078.

(67) Kirby, A.J. *Angew. Chem., Int. Ed. Engl.* **1996**, *35*, 707.

(68) (a) Nakano, S., Chadalavada, D. M., Bevilacqua, P. C. *Science* **2000**, *287*, 1493. (b) Weinger, J. S., Parnell, K. M., Dorner, S., Green, R., Strobel, S. A. *Nat. Struct. Mol. Biol.* **2004**, *11*, 1101.

(69) Bogie, P.M.; Holloway, L.R.; Ngai, C.; Miller, T.F.; Grewal, D.K.; Hooley, R.J. *Chem-Eur. J.* **2019**, *25*, 10232.

(70) (a) Hibbert, D. B.; Thordarson, P. *Chem. Commun.* **2016**, *52*, 12792. (b) Thordarson, P. *Chem. Soc. Rev.* **2011**, *40*, 1305.

(71) Ngai, C.; Bogie, P.M.; Holloway, L.R.; Dietz, P.C.; Mueller, L.J.; Hooley, R.J. *J. Org. Chem*, **2019**, *84*, 12000.

(72) Richter, M. *Nat. Prod. Rep.* **2013**, *30*, 1324.

(73) (a) Zhang, Q.; Tiefenbacher, K. *Nat. Chem.* **2015**, *7*, 197. (b) Zhang, Q.; Catti, L.; Pleiss, J.; Tiefenbacher, K.. *J. Am. Chem. Soc.* **2017**, *139*, 11482.

(74) (a) Pluth, M. D.; Bergman, R. G.; Raymond, K. N. *Science* **2007**, *316*, 85. (b) Cullen, W.; Misuraca, M. C.; Hunter, C. A.; Williams, N. H.; Ward, M. D. *Nat. Chem.* **2016**, *8*, 231. (c) Cullen, W.; Metherell, A. J.; Wragg, A. B.; Taylor, C. G. P.; Williams, N. H.; Ward, M. D. *J. Am. Chem. Soc.* **2018**, *140*, 2821–2828.

Biosketch

	Richard Hooley obtained his undergraduate degrees in Natural Sciences from Emmanuel College, Cambridge University, and his Ph.D. in the laboratory of Prof. Martin F. Semmelhack at Princeton. Following a postdoctoral position in the lab of Prof. Julius Rebek Jr. at The Scripps Research Institute in La Jolla, CA he began his independent career in the Department of Chemistry at the University of California – Riverside. The Hooley group works on various aspects of organic, inorganic and supramolecular chemistry, with a focus on the synthesis and applications of biomimetic self-assembled cages and hosts, and their functions in supramolecular catalysis, molecular recognition and biosensing.